Forced bursting and transition mechanism in CO oxidation with three time scales*

Li Xiang-Hong(李向红)[a)b)] and Bi Qin-Sheng(毕勤胜)[a)†]

[a)] Faculty of Civil Engineering and Mechanics, Jiangsu University, Zhenjiang 212013, China
[b)] Department of Mathematics and Physics, Shijiazhuang Tiedao University, Shijiazhuang 050043, China

(Received 26 August 2012; revised manuscript received 10 October 2012)

The mathematical model of CO oxidation with three time scales on platinum group metals is investigated, in which order gaps between the time scales related to external perturbation and the rates associated with different chemical reaction steps exist. Forced bursters, such as point–point type forced bursting and point–cycle type forced bursting, are presented. The bifurcation mechanism of forced bursting is novel, and the phenomenon where two different kinds of spiking states coexist in point–cycle type forced bursting has not been reported in previous work. A double-parameter bifurcation set of the fast subsystem is explored to reveal the transition mechanisms of different forced bursters with parameter variation.

Keywords: CO oxidation, forced bursting, bifurcation mechanism, enveloping slow-fast analysis

PACS: 05.45.–a, 82.40.Bj **DOI:** 10.1088/1674-1056/22/4/040504

1. Introduction

Many chemical oxidations involve multiple time scales, which often exhibit bursting oscillations[1,2] characterized by a combination of large amplitude oscillation and relatively small amplitude oscillation in each evolution process.[3,4] Bursting phenomena occur when the reaction alternates between a quiescent state (QS) and repetitive spikes (SPs), in which two important bifurcations can be observed: the bifurcation of a QS leading to repetitive SPs and bifurcation of SP to a QS.[5,6] Such an oscillation has been extensively studied in many fields, such as neuronal, chemical kinetics, electronic circuits, and population dynamics.[7–13]

Models with multiple time scales are often described by coupled ordinary equations with a fast subsystem (FS) and slow subsystem (SS).[14,15] By taking a slow variable as bifurcation of FS, the slow-fast analysis method can be widely used to reveal the bifurcation mechanism of the bursting phenomenon.[16–18] In our previous work, the enveloping slow-fast analysis method has been used to account for the dynamical mechanism of bursting with periodic perturbation, in which the bifurcation of FS, associated with two types of extreme cases for the variation of periodic excitation, has been introduced.[19] However, up to now, most of the work may refer to two time scales, while the bursting behavior related to three time scales is an open problem, especially when catalytic oxidations are involved. In this paper, we focus on the catalytic oxidation of CO over platinum-group metals for the case where there can be the existence of order gaps between the three time scales associated with periodic perturbation, a reaction rate in the subsurface layers and a reaction rate on the surface of the catalyst.

CO oxidation has attracted much attention due to its technological importance in the areas of pollution control and fuel cells.[20,21] A lot of research work has been done on the oxidation on platinum group metals, involving consistency for the mathematical micro- and macro-level models,[22] self-oscillation of the reaction rate accompanied by an auto-wave process,[23] and bursting and chaotic dynamics with consideration of the reconstructive heterogeneity of the surface and subsurface.[24]

Considering the catalytic reaction of CO oxidation on the platinum group metals based on the Langmuir–Hinshelwood mechanism, shown in Table 1, a three-variable scaled chemical mechanism may be described by the following dimensionless form[24]

$$\begin{aligned} x' &= K_1(1-x-y) - K_{-1}x - K_3xy, \\ y' &= 2K_2(1-x-y)^2 - K_3xy, \\ z' &= K_4y(1-z) - K_5xz = \varepsilon(\alpha y(1-z) - xz), \end{aligned} \tag{1}$$

where x and y represent the dimensionless concentrations of CO and O absorbed on the surface, respectively, and z denotes the dimensionless concentration of subsurface oxygen. Since the elementary reaction constants K_4 and K_5 are much smaller than $K_i, i = 1, -1, 2, 3$, this leads to the slow-fast system with two time scales.

Here, we introduce small periodic perturbation into system (1), and the variables of external excitation may change on the scale between the reaction rate in the subsurface layer and that on the surface of the catalyst. Rich bursting phenomena, including chaotically forced bursting, multi-periodically

*Project supported by the National Natural Science Foundation of China (Grant Nos. 20976075, 10972091, and 11002093) and the College Graduate Student Scientific Research Innovation Foundation of Jiangsu Province, China (Grant No. CXLX12-0619).

†Corresponding author. E-mail: qbi@ujs.edu.cn

© 2013 Chinese Physical Society and IOP Publishing Ltd

Table 1. Chemical scheme of the model of CO oxidation on the platinum group metals (cited from Ref. [24]), where the rate constants K_i ($i = -1, 1, 2, 3, 4, 5$) depend on partial pressure P_{CO} and P_{O_2}. R is the universal gas constant, 1 Torr = 1.33322×10^2 Pa.

Reactions	Rates	Parameters taken
$CO + Z \underset{K_{-1}}{\overset{K_1}{\rightleftharpoons}} ZCO$	$K_{-1} = 10^{13} \times \exp(-E_1/RT)$	$T = 500$ K
$O_2 + 2Z \xrightarrow{K_2} 2ZO$	$K_1 = 3.6 \times 10^5 P_{CO}$	$P_{O_2} = 9 \times 10^{-7}$ Torr
$ZCO + ZO \xrightarrow{K_3} CO_2 + 2Z$	$K_2 = K_{20} P_{O_2}$	$E_1 = 35$ K $\cdot$ cal $\cdot$ mol^{-1}
$ZO + Z_V \xrightarrow{K_4} Z_V O + Z$	$K_3 = 10^{13} \times \exp(-E_3/RT)$	$\varepsilon = 0.00003$
$ZCO + Z_V\ O \xrightarrow{K_5} CO_2 + Z_V + Z$	$\varepsilon = K_5,\ \alpha = K_4/K_5$	$\alpha = 4.65$

forced bursting, and periodically forced bursting, can be found. Furthermore, the enveloping slow-fast method and double-parameter bifurcation analysis may be used to explore the mechanism of forced bursting oscillations as well as the dynamical evolution of the system.

2. Mathematical model

Based on the experimental research, E_3 and K_{20} are determined by using the experimental data[24] shown in Table 1. For convenience to the theoretical analysis related to dynamics, the changes in E_3 and K_{20} can be approximated by piecewise linear functions as follows:

$$E_3 = \begin{cases} E_{31}, & y \le y_c - \delta, \\ \overline{E}_{32}, & |y - y_c| < \delta, \\ E_{33}, & y \ge y_c + \delta, \end{cases}$$

$$K_{20} = \begin{cases} K_{21}, & z \le z_c - \delta_1, \\ \overline{K}_{22}, & |z - z_c| < \delta_1, \\ K_{23}, & z \ge z_c + \delta_1, \end{cases} \tag{2}$$

where $y_c = z_c = 0.5$, $\delta = \delta_1 = 0.1$, $K_{21} = 0.9 \times 10^5$ s$^{-1} \cdot$ Torr^{-1}, $K_{23} = 0.11 \times 10^5$ s$^{-1} \cdot$ Torr^{-1}, $E_{31} = 28$ K $\cdot$ cal/mol, $E_{33} = 33$ K $\cdot$ cal/mol, $\overline{K}_{22} = (-39.5 \times z + 24.8) \times 10^4$ s$^{-1} \cdot$ Torr^{-1}, and $\overline{E}_{32} = 25y + 18$ K $\cdot$ cal/mol.

In this paper, a small periodic perturbation $a\cos\omega t$ is introduced, which may affect the change in the dimensionless concentration of CO absorbed on the surface, leading to the modified model, which is written as

$$\begin{aligned} x' &= K_1(1-x-y) - K_{-1}x - K_3xy + a\cos\omega t, \\ y' &= 2K_2(1-x-y)^2 - K_3xy, \\ z' &= \varepsilon(\alpha y(1-z) - xz). \end{aligned} \tag{3}$$

Since the ε parameter is very small, the full system can be divided into slow and fast subsystems, where x and y model the fast subsystem (FS), z describes the slow subsystem (SS), while external perturbation based on suitable frequency will change on the time scale between FS and SS. The dynamics with three time scales may interact with each other to exhibit rich nonlinear behavior, especially various types of forced bursters, which will be described in the following.

3. Bifurcation analysis

Obviously, $a\cos\omega t \in [-a, a]$. We introduce the model with constant perturbation written as

$$\begin{aligned} x' &= K_1(1-x-y) - K_{-1}x - K_3xy + p, \\ y' &= 2K_2(1-x-y)^2 - K_3xy, \\ z' &= \varepsilon(\alpha y(1-z) - xz), \end{aligned} \tag{4}$$

where $p = \pm a$, and the bifurcation details of FS in Eq. (4) may help to reveal the oscillation mechanism in the periodic perturbation system.

3.1. Fold bifurcation analysis

Since the piecewise-linear function involves the coefficient. Here, we only consider the case of $0 < y < 0.4$, and $0.4 < z < 0.6$. The relevant equations of FS can be written in the following form

$$\begin{aligned} x' &= f_1(x,y) = K_1(1-x-y) - 0.00504x - 5.78xy + p, \\ y' &= f_2(x,y) = (-0.711z + 0.4464)(1-x-y)^2 - 5.78xy. \end{aligned} \tag{5}$$

The steady state of FS, i.e. the equilibrium point $E_0(x_0, y_0)$, can be obtained by setting $x' = y' = 0$, which can yield

$$\begin{aligned} x_0 &= -\frac{12500(-K_1 + K_1y_0 - p)}{63 + 12500K_1 + 72250y_0}, \\ y_0^4 &+ a_1y_0^3 + a_2y_0^2 + a_3y_0 + a_4 = 0, \end{aligned} \tag{6}$$

where

$$\begin{aligned} a_1 &= -1.998 + K_1/r, \\ a_2 &= 0.99651 + 0.34602p + \frac{-K_1 + 0.173K_1^2}{r} - \frac{p}{r}, \\ a_3 &= 0.0017424 - 0.345719p \\ &\quad + \frac{-0.173K_1^2 - 0.173pK_1 - 0.00087K_1 - 0.00087p}{r}, \\ a_4 &= 0.76 \cdot 10^{-6} - 0.0003017p + 0.0299326p^2, \\ r &= -0.711z + 0.4464. \end{aligned}$$

Assuming $y_0 = u - b_1/4$, equation (6) can be transformed into

$$u^4 + b_1u^2 + b_2u + b_3 = 0. \tag{7}$$

Let $A = b_1^2 + 12b_3$, $B = 9b_2^2 + 2b_1(b_1^2 - 4b_3)$, $C = 6b_1b_2^2 + (b_1^2 - 4b_3)^2$, $\Delta = B^2 - 4AC$. If $\Delta = 0$ and $B \neq 0$, one double-root can exist in Eq. (7), then the fold bifurcation may take place in the FS.

3.2. Hopf bifurcation analysis

For $0.4 < z < 0.6$ and $0.4 < y < 0.6$, the FS of system (4) can be described as

$$\begin{aligned} x' &= f_1(x,y,z) = K_1(1-x-y) - 0.00504x \\ &\quad - 10^{13}xy\exp(-1.0064(25y+18)) + p, \\ y' &= f_2(x,y,z) = (-0.711z + 0.4464)(1-x-y)^2 \\ &\quad - 10^{13}xy\exp(-1.0064(25y+18)). \end{aligned} \tag{8}$$

The steady mode of the reaction, i.e., the equilibrium point, denoted by $E_0(x_0, y_0)$, of the vector field can be obtained by setting $x' = y' = 0$ and solving the two resulting algebraic equations, of which the stabilities can be determined by the eigenvalues of the characteristic polynomial associated, and written in the following form

$$p(\lambda) = \begin{vmatrix} a_{11} - \lambda & a_{12} \\ a_{21} & a_{22} - \lambda \end{vmatrix} = \lambda^2 + p_1\lambda + p_2, \tag{9}$$

where

$$\begin{aligned} s &= \exp(-1.0064(25y_0 + 18)), \\ a_{11} &= -K_1 - 0.00504 - 10^{13}y_0 s, \\ a_{12} &= -K_1 - 10^{13}x_0 s + 0.2516 \cdot 10^{15}x_0y_0 s, \\ a_{21} &= -2r(1-x_0-y_0) - 10^{13}y_0 s, \\ a_{22} &= -2r(1-x_0-y_0) - 10^{13}x_0 s + 0.2516 \cdot 10^{15}x_0y_0 s, \\ p_1 &= 2(1-x_0-y_0)r + 10^{13}(x_0 + y_0 - 25.16 \cdot x_0y_0)s + K_1, \\ p_2 &= 10^{13}(x_0 + y_0 - 25.16 \cdot x_0y_0)sK_1 \\ &\quad + 10^{13}(50.32x_0^2y_0 + 2y_0 + 2x_0^2 + 50.32x_0y_0^2 \\ &\quad - 2y_0^2 - 2x_0 + 50.32x_0y_0)sr + 0.01008(1-x_0-y_0)r \\ &\quad + 10^{13}(0.00504 - 0.1268y_0)x_0 s. \end{aligned}$$

By using the Routh–Huwitz criterion, the equilibrium point E_0 is stable if

$$p_1 < 0, \quad p_2 > 0. \tag{10}$$

Based on transversal conditions, $\mathrm{Re}(\mathrm{d}\lambda/\mathrm{d}z)_{E_0} = 1.422(1 - x_0 - y_0) \neq 0$, Hopf bifurcation sets can be expressed as $p_1 = 0$, $p_2 > 0$, and $x_0 + y_0 < 1$.

4. Forced bursting and bifurcation mechanism

For the fixed excitation amplitude $a = 0.0014$ and frequency $\omega = 0.0095$, the whole model with three time scales can be written as

$$\begin{aligned} x' &= K_1(1-x-y) - K_{-1}x - K_3xy + 0.0014\cos 0.0095t, \\ y' &= 2K_2(1-x-y)^2 - K_3xy, \\ z' &= K_4y(1-z) - K_5xz = \varepsilon(\alpha y(1-z) - xz), \end{aligned} \tag{11}$$

of which the dynamics with a variation in the K_1 parameter would be revealed in the following.

4.1. Point–point type forced bursting

For the K_1 parameter fixed at 0.0351, periodic bursting exists in the system, which is plotted in Fig. 1. One may find that the whole trajectory is divided into three parts. The first part is the SP between A and B characterized by relatively large amplitude oscillation, the second part between C and D may be in a rest state or exhibit small amplitude oscillation, called QS, and the last is two times the jumping behavior, which may lead to the alternation between SP and QS.

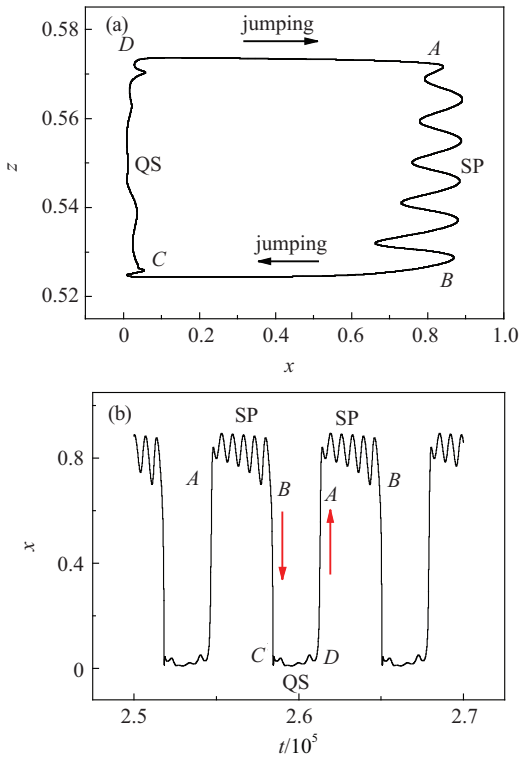


Fig. 1. (color online) For $K_1 = 0.0351$, (a) the phase portrait on the xoz plane, and (b) the time history.

It is noted that the value of the perturbation $0.0014\cos 0.0095t$ in Eq. (11) may change between $p_1 = 0.0014$ and $p_2 = -0.0014$. Based on the enveloping slow-fast analysis method and by taking the slow variable z as a bifurcation parameter, the bifurcation details of FS can be plotted in Fig. 2(a). For $p = p_2 = -0.0014$, the equilibrium curves of FS are denoted by LN, where $N1$, $N2$ are critical points of fold bifurcation, and the equilibrium points between $N1$ and $N2$ are unstable, while equilibria located on $N1$–NA and $N2$–NB are stable. LP represents the equilibrium curves of FS for $p = p_1 = 0.0014$, on which $P1$ and $P2$ are critical points of fold bifurcation, and the unstable equilibria are only located on the curve between two fold bifurcation points, $P1$ and $P2$.

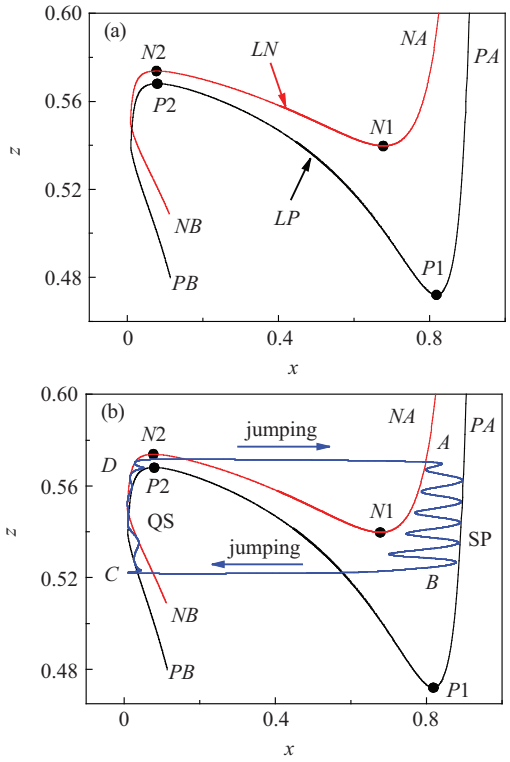


Fig. 2. (color online) For $K_1 = 0.0351$, (a) the bifurcation analysis of FS, and (b) the overlap of the bifurcation diagram with phase portrait.

To explore the bifurcation mechanism of the burster, we overlap the bifurcation diagram and the phase portrait on the *xoz* plane as shown in Fig. 2(b). We can check that both the SP and QS of the trajectory are fully confined to the two stable equilibrium curves, which indicates that the attraction of two stable equilibrium curves may lead the trajectory to oscillation. It is obvious that the region between *NA*–*N*1 and *PA*–*P*1 is wide enough for the system to oscillate with large amplitude according to periodically forced frequency, leading to SP. On the other hand, because the region between *NB*–*N*2 and *PB*–*P*2 is very narrow, the trajectory can vibrate with small amplitude or be in a rest state, resulting in QS. Furthermore, the fold bifurcation of FS guides the alternation between SP and QS, and the turning point of the two-time jumping phenomena may be confined to the bifurcation points of FS. We call this point–point type forced periodic bursting.

When the values of parameter K_1 are taken to be 0.024567 and 0.024978, respectively, four-period bursting and chaotic bursting can be observed, of which the phase portrait and bifurcation details are presented in Fig. 3. We can find that all the trajectories behaving in SPs may be located in a wide region between two stable equilibrium curves, while the OS of the system is confined in a narrow region, so the two kinds of phenomena can be called point–point type forced multi-periodically bursting and point–point type forced chaotic bursting, respectively. Here we should point out that all of the turning points related to the jumping behavior in both the forced multi-periodically and forced chaotic bursting oscillations may be fully restricted by critical fold bifurcation points in FS.

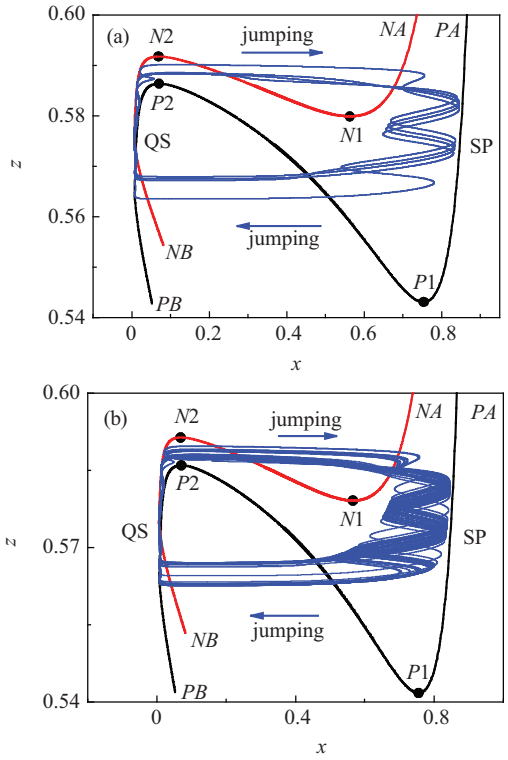


Fig. 3. (color online) Overlap of the bifurcation diagram with phase portrait for (a) $K_1 = 0.024567$ and (b) $K_1 = 0.024978$.

4.2. Point–cycle type forced bursting

For the K_1 parameter fixed at 0.045, another type of bursting oscillation may appear in the system with three time scales, as shown in Fig. 4(a). It is clear that two different kinds of SSs, denoted SP1 and SP2, respectively, exist in the periodic trajectory. To further reveal the mechanism of the system, figure 4(b) exhibits the details of the bifurcation of FS, where there exists supercritical point H of Hopf bifurcation in FS with $p = p_2 = -0.0014$.

By using the enveloping slow-fast analysis method, the overlaying diagram of Fig. 4(a) with Fig. 4(b)) is shown in Fig. 4(c). Note that the stable limit cycles generated by supercritical Hopf bifurcation of FS may result in the large amplitude oscillations of the trajectory to form SP1, while SP2 is caused by external periodic excitation together with the tendency to two stable equilibrium curves, and the coexistence of the equilibrium attractor and limit cycle attractor of FS may guide the transition between SP1 and SP2. Here we should point out that the oscillation frequency in SP1 is determined by Hopf bifurcation of FS, while the trajectory in SP2 may oscillate with excitation frequency. Therefore, the burster with SP1, SP2, and QS can be called point–cycle type forced periodic bursting, which is the typical nonlinear dynamic behavior of a system with three time scales.

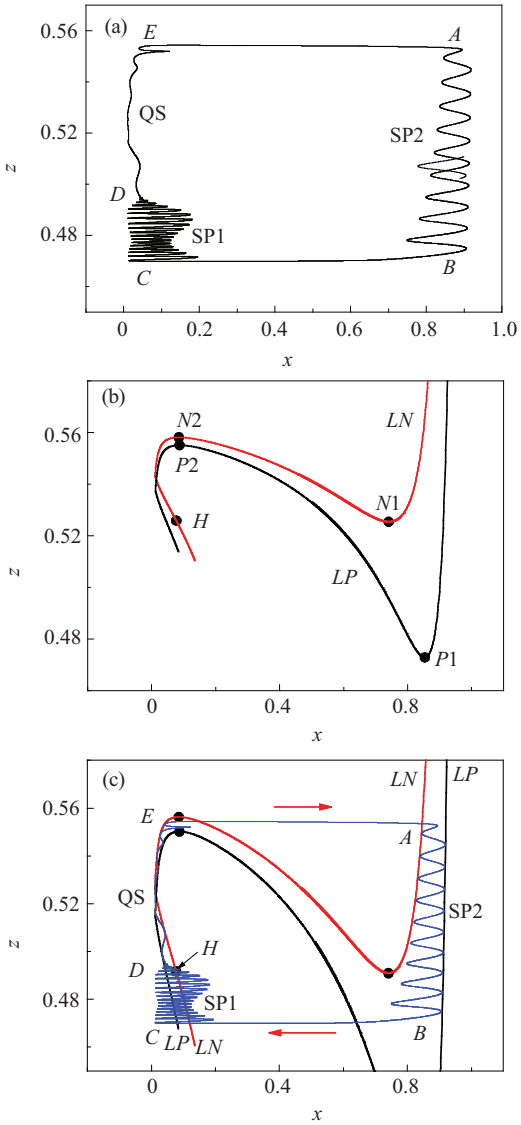


Fig. 4. (color online) For $K_1 = 0.045$, (a) the phase portrait, (b) the bifurcation analysis of FS, and (c) the overlap of the phase portrait with the bifurcation diagram.

5. Transition mechanism for two types of forced bursting

In this section, we turn to the investigation of the transition mechanism between different bursting patterns with the variation of parameter K_1. By taking K_1 and the slow variable z as the bifurcation parameters, the bifurcation sets of FS are presented in Fig. 5, where $LN1$, $LN2$, and $LP1$, $LP2$ represent the fold bifurcation sets of Eq. (5) for $p = -0.0014$ and $p = 0.0014$, respectively, while LH denotes the supercritical Andronv–Hopf bifurcation sets of Eq. (8) for $p = -0.0014$. For example, when $K_1 = 0.045$, all of the bifurcation points $N1$, $N2$, $P1$, $P2$, and H plotted in Fig. 4(b), are located at the bifurcation sets $LN1$, $LN2$, $LP1$, $LP2$, and LH, respectively. The intersection points of LH with both $LN1$ and $LP1$ are denoted by $S1$ and $S2$, respectively, with the parameter values $(K_1, z)_{S1} \approx (0.02585, 0.5356)$ and $(K_1, z)_{S2} \approx (0.04785, 0.475)$.

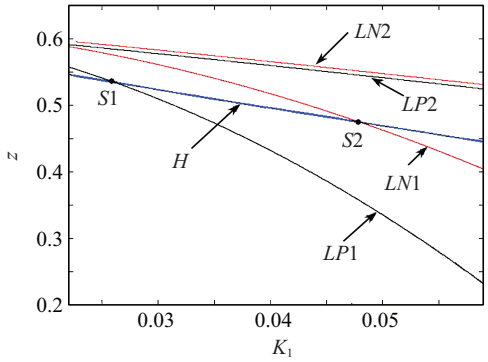


Fig. 5. (color online) Bifurcation sets of FS with respect to the slow variable z and K_1 for $p = \pm 0.0014$.

It can be checked that when K_1 is taken left to $S1$, i.e. $K_1 < 0.02585$ (see Fig. 5), them the Andronv–Hopf bifurcation curve LH is located below all of the fold curves, which implies that the trajectory can only go through the fold bifurcation of FS, and then the burster of the system may be point–point type forced bursting. While when K_1 is taken right to $S2$, i.e. $K_1 > 0.04785$, then the supercritical Hopf bifurcation curve H is located between curve $LN1$ and $LP2$, which leads to the trajectory involved in both the Hopf and fold bifurcations, so the bifurcation mechanism of the burster may be point–cycle type forced bursting. Therefore, the transition of two kinds of bursters must take place between $S1$ and $S2$.

To further explore the transition of the bursting patterns, by taking $x = 0.35$ as the cross section, the Poincare maps of all the trajectories for $K_1 \in (0.02, 0.058)$ are plotted in Fig. 6(a), which is divided into two branches. It should also be mentioned that all of the points on the cross section may record z-values at all of the turning points of the jumping behavior, which can be checked by Figs. 1–4. By overlapping the Poincare map with the bifurcation sets of FS, figure 6(b) can be obtained, where the upper branch of the Poincare map may be fully enveloped by the fold bifurcation sets $LN2$ and $LP2$, while the lower branch is located between the fold bifurcation sets $LN1$ and $LP1$. This phenomenon is in common with all the jumping behaviors of the forced bursters observed in Section 4.

Now we continue to focus on the transition of the bursting mechanism between $S1$ and $S2$, i.e. $0.02585 < K_1 < 0.04785$ (see Fig. 6(b)). Note that curve LH and the Poincare map intersect at point M (0.0391, 0.4985), which causes limit cycles to occur for $K_1 > 0.0391$. For $K_1 < 0.0391$, although Hopf bifurcation exists for FS, the trajectory of the full system is involved only in the fold bifurcation of FS because of the critical point of Hopf bifurcation below the turning points of the jumping behavior. For $K_1 > 0.0391$, the critical point of Hopf bifurcation in FS may appear between two-time jumping, which leads to the fact that the trajectory of the system may be involved in two kinds of bifurcations. Therefore, with the increase in parameter K_1, point–point type forced bursting

related to fold bifurcation of FS may evolve into point–cycle type forced bursting associated with both fold and Hopf bifurcations, while point M is the turning point of the transition mechanism.

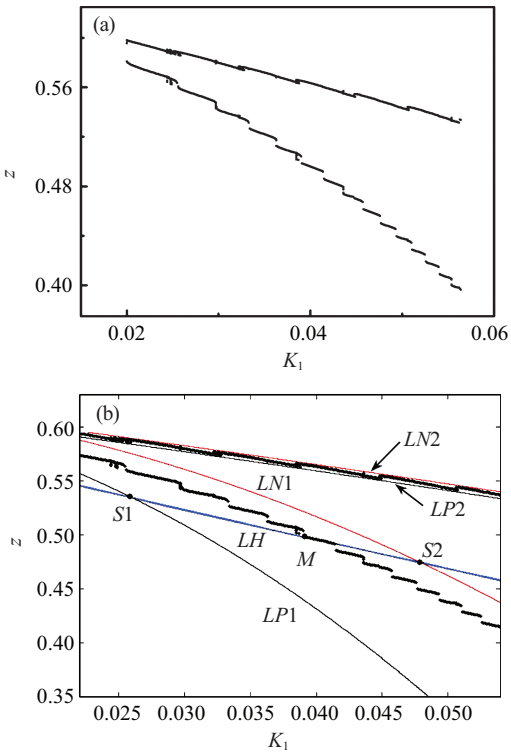


Fig. 6. (color online) (a) Poincare map and (b) overlap of the bifurcation diagram of FS with the Poincare map.

6. Conclusion

Because of the order gaps between weak periodic perturbation, reaction rates in the subsurface and on the surface, the system in CO oxidation on platinum group metals may behave on three time scales. Rich dynamical behavior, such as point–point type forced bursting and point–cycle type forced periodic bursting, is observed. The characteristic feature of forced bursting is that the large amplitude oscillation according to excitation frequency, confined to a wide region between two stable equilibrium curves of FS, forms the SP in the whole trajectory, while the narrow region between two stable equilibrium curves of FS leads the system to QS, presenting small amplitude oscillations or a rest state. When Hopf bifurcation is involved, there are two types of SPs in point–cycle type forced periodic bursting, and the induced mechanism of the two types of SPs may be completely different.

Furthermore, with a parameter increase, point–point type forced bursting can evolve into point–cycle type forced bursting. The relevant bifurcation mechanism based on double-parameter analysis of FS shows that the bursting pattern depends on the positional relation between the Hopf and fold bifurcation points. By overlapping the bifurcation sets with a Poincare map, not only can the phenomenon that all the jumping behaviors of the forced bursters can be controlled by critical points of the fold bifurcation of FS be verified, but the turning point of the transition between different types of forced bursting can also be found. Therefore, from the view of bifurcation, we can predict and control the complex nonlinear behavior of CO oxidation on platinum group metals.

References

[1] Gyorgyi L and Field R J 1992 *Nature* **355** 808
[2] Li Q S and Zhu R 2004 *Chaos, Solitons and Fractals* **19** 195
[3] Davis M J and Klippenstein S J 2002 *J. Phys. Chem. A* **106** 5860
[4] Mease K D 2005 *Appl. Math. Comput.* **164** 627
[5] Fujimoto F and Kaneko K 2003 *Physica D* **180** 1
[6] Conforto F, Groppi M and Jannelli A 2008 *Appl. Math. Comput.* **206** 892
[7] Lu Q S, Yang Z Q, Duan L X, Gu H G and Ren W 2009 *Chaos, Solitons and Fractals* **40** 577
[8] Bi, Q S 2010 *Sci. China E: Tech. Sci.* **53** 748
[9] Savino G V and Formigli C M 2009 *BioSystems* **97** 9
[10] Vidal A 2006 *Positive Systems, LNCIS* **341** 439
[11] Butera R J Jr, Rinzel J and Smith J C 1999 *J. Neurophysiol.* **82** 382
[12] Zhou G H, Xu J P, Bao B C, Zhang F and Liu X S 2010 *Chin. Phys. Lett.* **27** 090504
[13] Song M, Wang B N and Xu G S 2003 *Chin. Phys.* **12** 189
[14] Perc M and Marhl M 2003 *Chem. Phys. Lett.* **376** 432
[15] Surana A and Haller G 2008 *Physica D* **237** 1507
[16] Duan L X, Lu Q S and Cheng D Z 2009 *Sci. China E: Tech. Sci.* **52** 771
[17] Terman D 1992 *J. Nonlinear Sci.* **2** 135
[18] Han X J and Bi Q S 2009 *Acta Phys. Sin.* **58** 4408 (in chinese)
[19] Li X H and Bi Q S 2012 *Chin. Phys. B* **21** 060505
[20] Kummer J T 1986 *J. Phys. Chem.* **90** 4747
[21] Armor J N 1999 *Appl. Catal. A* **176** 159
[22] Kurkina E S and Semendyaeva N L 2003 *Comput. Math. Modeling* **14** 319
[23] Latkin E I, Elokhin V I and Gorodetskii V V 2001 *J. Mol. Catal. A: Chem.* **166** 23
[24] Lashina E A, Chumakova N A, Chumakov G A and Boronin A I 2009 *Chem. Eng. J.* **154** 82